PAPER

Check for updates

Graphitic carbon nitride and APTES modified advanced electrochemical biosensor for detection of 17β-estradiol in spiked food samples

M. S. Bacchu,[ab] M. R. Ali,[ab] M. N. Hasan,[ab] M. R. A. Mamun,[ab] M. I. Hossain [ID] [ab] and M. Z. H. Khan [ID] *[ab]

This work demonstrates a simple and inexpensive electrochemical biosensing pathway for selective and sensitive recognition of 17β-estradiol (E2) in environmental and food samples. The biosensing system is based on graphitic carbon nitride (g-C$_3$N$_4$) and a conductive polymer 3-aminopropyltriethoxysilane (APTES). The proposed biosensor shows the ability to detect E2 in attomolar levels within a wide linear logarithm concentration range of 1×10^{-6} to 1×10^{-18} mol L^{-1} with a limit of detection (LOD) of 9.9×10^{-19} mol L^{-1}. The selectivity of the developed biosensor was confirmed by conducting the DPV of similarly structured hormones and naturally occurring substances. The proposed biosensor is highly stable and applicable to detect E2 in the presence of spiked food and environmental samples with satisfactory recoveries ranging from 95.1 to 104.8%. So, the designed electrochemical biosensor might be an effective alternative tool for the detection of E2 and other endogenous substances to attain food safety.

1 Introduction

In recent years, food concern has been raised due to various environmental polluted endocrine-disrupting chemicals (EDCs). EDCs have the potential to create an environmental hazard by jeopardizing the ecological balance.[1] The primary female sex hormone 17β-estradiol (E2) has played a vital role in the enrichment of EDCs. E2 is the smallest natural estrogen steroid hormone which is very important for the development and regulation of the female reproductive tissues such as the thorax, uterus, intestinal motility, and vagina during puberty, adulthood, and majority of pregnancy.[2,3] Naturally occurring conjugates of estrogens have become a new problem in the food industry owing to the environmental disrupting physiological effects of the hormones.[4] Among these natural environmental estrogens, E2 is substantially more potential than prime metabolites estriol (E3) and estrone (E1). E2 is used widely in the feed processing industry illegally to promote animal growth activity, milk yield, the ratio of fatty meat of cattle and poultry.[1,5,6] Although E2 does some crucial works in the female body, E2 carries several adverse effects such as a tumor, breast cancer, endocrine disorder, abnormal cell growth, *etc.* when it enters the human body due to food chain contamination.[7] In particular, the high activity of E2, even at a very low

concentration thus can be toxic and carcinogenic.[8,9] Therefore, quantitative, reliable, sensitive, real-time, inexpensive, and rapid detecting tools for E2 are vitally important in the fields of food safety and health protection.

Nowadays, a large number of advanced techniques has been developed for the quantification of E2 in food and environmental fields, such as enzyme-linked immunosorbent assay (ELISA),[10] high-performance liquid chromatography (HPLC),[11,12] UV-vis spectrophotometry,[2] capillary electrophoresis,[13] Gas Chromatography-Mass Spectrometry (GCMS).[14] In practical application, these methods contain some drawbacks such as time-consuming, highly expensive, unsatisfactory detection limit and sensitivity, complex pre-treatment process, and requirement of trained operators.[15,16] To overcome these obstacles, electrochemical biosensing system are highly recommended by many researcher group in recent years.

Moreover, in recent years the electrochemical biosensor is one of the promising methods which become popular due to fast response, inexpensive, easy to perform, and real-time detection, *etc.*[16,17] Nano-particle and conductive polymer are widely used in electrochemical biosensing platform to enhance selectivity, sensitivity, bio-compactability, and active sensing surface area, *etc.*[18] Graphitic carbon nitride (g-C$_3$N$_4$) is nitrogen and carbon rich polymeric semiconductor offers some special properties such as medium band gab (2.7 eV), low toxicity, easy preparation, larger surface area, and high electrocatalytic properties *etc.*[19,20] The g-C$_3$N$_4$ is widely used in fabrication of electrochemical biosensor to detect biomolecules and boost the electrochemical performance of the biosensor.[21] In literature,

[a]*Dept. of Chemical Engineering, Jashore University of Science and Technology, Jashore 7408, Bangladesh. E-mail: zaved.khan@yahoo.com*

[b]*Laboratory of Nano-bio and Advanced Materials Engineering (NAME), Jashore University of Science and Technology, Jashore 7408, Bangladesh*

Yola et al., for very first time developed an molecular imprinted sensor based on g-C$_3$N$_4$ for determination of melamine in food sample.[22] Recently, Silva et al., represents g-C$_3$N$_4$ nanosheet based electrochemical sensor for monitoring hydroxychloroquine sulfate in urine and pharmaceutical formulation sample.[21] The pioneeror group reported g-C$_3$N$_4$ increase the surface conductivity of electrode and recognition ability of designed biosensor. APTES is a conductive polymer is widely used in different biosensing platform to enhance electrocatalytic properties of biosensor.[23,24]

In this work, we have reported g-C$_3$N$_4$ and APTES modified electrochemical biosensor for selective recognition of E2. Different surface topographical analysis such as ATR-FTIR, SEM were carried out to confirm interaction between APTES and g-C$_3$N$_4$. The voltametric behaviours of the developed biosensor were investigated through CV, DPV, and EIS. The biosensor is capable to detect E2 at the attomolar level in food and environmental sample.

2 Experiment

2.1 Apparatus

An electrochemical workstation Corrtest CS300 (China) was used to conduct all voltammetric measurements. Electrochemical impedance spectroscopy (EIS) data were obtained from a Metrohm DropSens μStat-i 400s (Switzerland). A conventional three-electrode system was used to conduct all measurements which consist of a different modified screen-printed electrode (SPE) (3 mm in diameter) as the working electrode, platinum wire as the auxiliary electrode, Ag/AgCl as the reference electrode. The surface topography of different modified electrodes materials was investigated by using ZEISS Gemini SEM 500 (UK) and NICOLET iS20 Attenuated total reflectance-Fourier transform infrared (ATR-FTIR) spectroscopy (Germany). All voltammetric experiments were executed at room temperature at N$_2$ atmosphere.

2.2 Chemicals and reagents

17β-Estradiol (E2) and 3-aminopropyltriethoxysilane (APTES) were obtained from Aladdin Biochemical Technology Co. Ltd (China). Thiourea (CH$_4$N$_2$S), trichloroacetic acid, potassium ferrocyanide (K$_4$[Fe(CN)$_6$]), potassium ferricyanide (K$_3$[Fe(CN)$_6$]), potassium chloride (KCl), and other reagents were parched from Merck (India). For electrochemical measurement, a supporting electrolytic solution was used for all electrochemical measurement purposes which were made of 5 × 10^{-3} mol L^{-1} (K$_4$[Fe(CN)$_6$]), (K$_3$[Fe(CN)$_6$]) and 0.1 mol L^{-1} KCl. Food samples of water, milk, and poultry meat were purchased from a local market. Ultrapure water (Type I) produced from Evoqua was used to prepare all working solutions (Germany, resistivity < 18 MΩ).

2.3 Synthesis of graphitic carbon nitride (g-C$_3$N$_4$)

The graphitic carbon nitride (g-C$_3$N$_4$) was typically synthesized using the solvent assist method[25] with minor modification. In short, 12 g of thiourea was dissolved in 30 mL of absolute ethanol in a semi-closed crucible. The solution was directly calcined in a muffle furnace at 550 °C for 2 h at a heating rate of 5 °C min^{-1} and then naturally cooled to room temperature. The obtained powder was collected for further use.

2.4 Fabrication of APTES/g-C$_3$N$_4$/SPE

The screen-printed electrode (SPE) surface was washed ultra-pure water and dried at room temperature under nitrogen (N$_2$) gas. After that, a 10 μL aliquot of 1 mg mL^{-1} prepared g-C$_3$N$_4$ suspension was drop-casted onto the working electrode of the SPE-activated surface, and then dried at N$_2$ gas. Eventually, we eagerly followed a similar method for APTES modification, which was reported previously work.[23] In short, the working electrode was rinsed thoroughly with ultrapure water and immersed in a solution of H$_2$O/NH$_4$OH/H$_2$O$_2$ (5 : 1 : 1) for 30 min, and then dried at 60 °C to hydroxylate active g-C$_3$N$_4$/SPE surface. Subsequently, the electrode was further rinsed with ultrapure water and also immersed in APTES with 2% ethanol solution for 60 min, and also dried at 70 °C. Finally, the electrodes were carefully rinsed ultrapure water, and then dried at room temperature. Then modified electrode (APTES/g-C$_3$N$_4$/SPE) was stored at 4 °C for further used.

2.5 Electrochemical measurement techniques

The electrochemical behavior was measured using different modified electrodes in the probe solution which was carried out in 0.1 M KCl containing 5 mM [Fe(CN)$_6$]$^{3-/4-}$ solution at a potential range from −0.2 V to +0.6 V with a scan rate of 50 mV and pulse period of 0.1 s. The difference of the DPV response was determined by subtracting the oxidation peak potential of [Fe(CN)$_6$]$^{3-/4-}$ with and without binding E2. Electrochemical impedance spectroscopy (EIS) was conducted in the same solution containing a frequency range of 0.1 Hz to 100 000 Hz and an amplitude of 10 mV. Scheme 1 depicts step by step procedure for fabrication of the biosensor and detection of E2.

### 2.6 Pre-treatment of real samples

The preparation of a real sample was described in our previous work.[26] In short, 2 g of milk, water, and poultry meat sample was taken into a polypropylene tube with 10 ml trichloroacetic acid (10% w/v) and vertexed for 2 min. The supernatant was separated by Whatman filter paper to obtain a fresh solution after centrifuging for 15 min at 5000 rpm respectively. These solutions were diluted 100 times with 5 × 10^{-3} mol L^{-1} [Fe(CN)$_6$]$^{3-/4-}$ at a pH of 7.0 for further application.

3 Result and discussion

3.1 Surface topography of the modified biosensor

The surface topography of different modified electrodes were investigated through SEM, ATR-FTIR which is shown in (Fig. 1). Fig. 1A shows the SEM image of g-C$_3$N$_4$/SPE which confirmed a sheet like g-C$_3$N$_4$ successfully incorporate on the surface of SPE. Fig. 1B shows the SEM image of APTES on the surface of g-C$_3$N$_4$/SPE. EDX of g-C$_3$N$_4$ with percentage of different element present in g-C$_3$N$_4$ is shown in Fig. 1C. The functional group
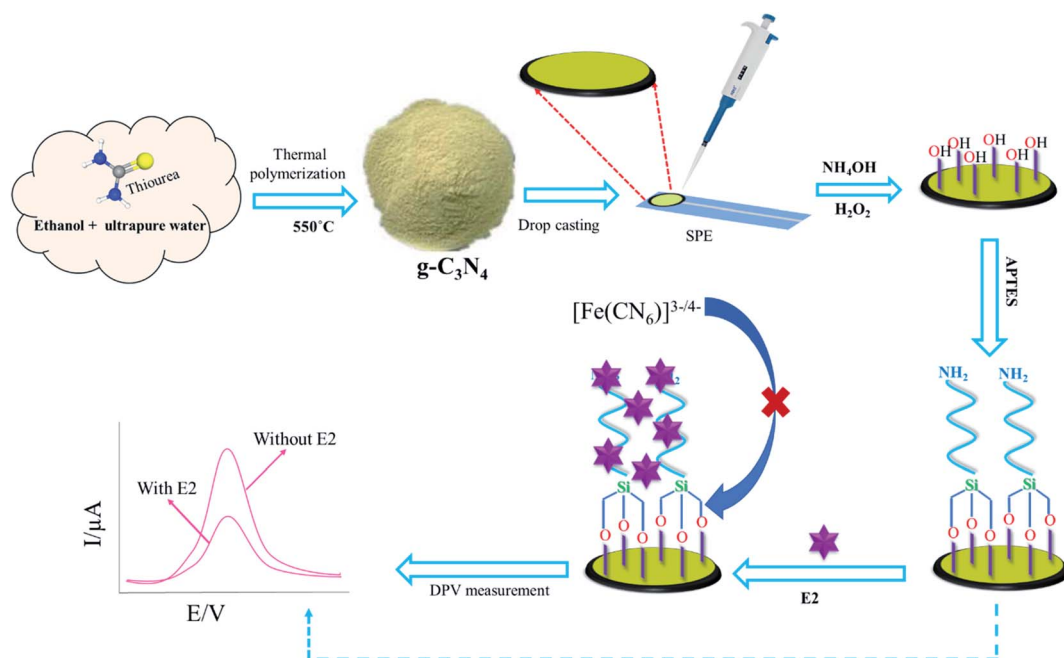
Scheme 1 Systematic procedure to fabricate the proposed biosensor and detection of E2.

analysis of g-C$_3$N$_4$, g-C$_3$N$_4$/APTES, g-C$_3$N$_4$/APTES/E2 were conducted through FTIR (Fig. 1D). The FTIR spectra of g-C$_3$N$_4$ shows a series of intense band at 1410, 1570, 1641 cm^{-1} for C–N stretching vibration which confirmed successful synthesis of g-C$_3$N$_4$. The bands at 1320 and 1240 cm^{-1} were assigned to C–

NH–C stretching vibration. The presence of s-triazine unit in out-of-plane of g-C$_3$N$_4$ was confirmed by a sharp peak at 806 cm^{-1}.[27,28] After conjugation of APTES with g-C$_3$N$_4$, the intensity of s-triazine ring got weaker after conjugation of APTES suggesting APTES successfully bind with g-C$_3$N$_4$ by
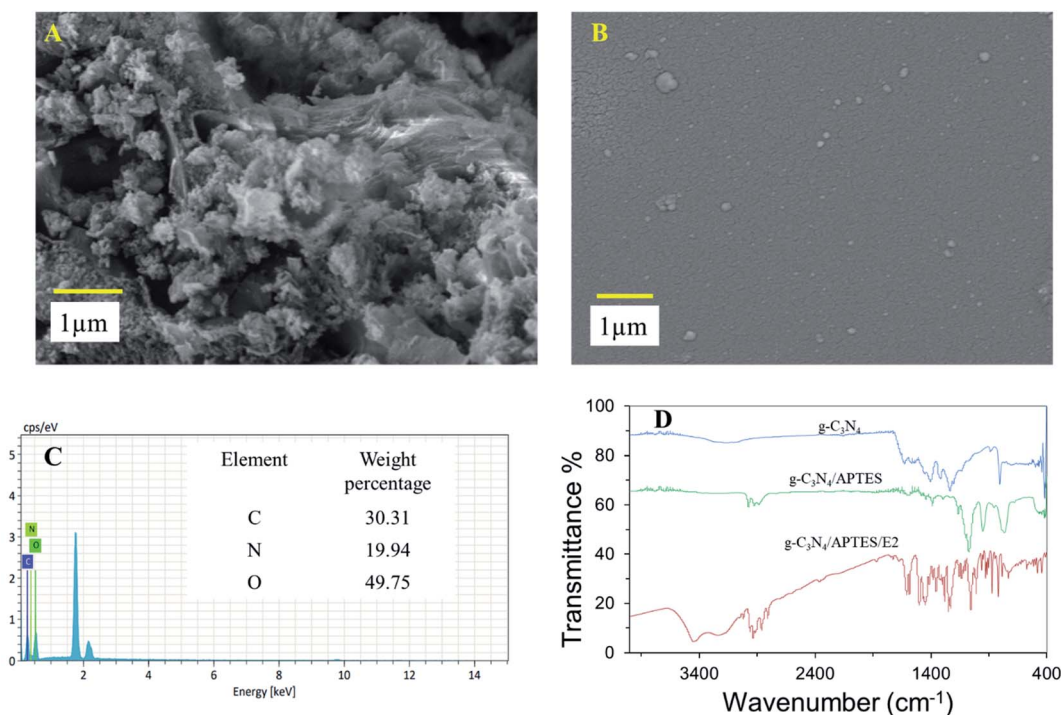

Fig. 1 SEM image of g-C$_3$N$_4$/SPE (A), g-C$_3$N$_4$/APTES/SPE (B); EDX analysis of g-C$_3$N$_4$/SPE (C) and FTIR spectra of g-C$_3$N$_4$, g-C$_3$N$_4$/APTES, g-C$_3$N$_4$/APTES/E2 (D).

intermolecular interaction. Other peaks were found at 1580 cm^{-1} for N–H, 1290 and 765 cm^{-1} for Si–C, and 1165 and 765 cm^{-1} for Si–O–C which confirmed presence of APTES on the surface of g-C$_3$N$_4$.[28] The FTIR analysis of g-C$_3$N$_4$/APTES/E2 shows some similarity in peak intensity and shifting which indicates E2 interact with g-C$_3$N$_4$/APTES. Some intense peak was found at 3449, 1342 and 1230 cm^{-1} for –OH, C–O and –CH$_2$ due to addition of E2.[29]

3.2 Electrochemical behavior of modified electrodes

To assess the electrochemical properties of different modified electrodes, cyclic voltammetry (CV) and electrochemical impedance spectroscopy (EIS) were carried out. Fig. 2A represents the cyclic voltammogram of the different modified electrodes in the supporting electrolyte at a scan rate of 50 mV s^{-1} in a potential range of −0.2 V to 0.6 V. To compare the electron transfer kinetics of different modified electrodes, the difference between oxidation and reduction peak potential ($\Delta E_p = E_{pc} - E_{pa}$) was calculated. Fig. 2A depicts the bare SPE exhibited ΔE_p value of 130 mV suggesting a poor electron transfer rate.[30] Surprisingly, the ΔE_p value was significantly decreased (108 mV) after drop-casting g-C$_3$N$_4$ on the surface of SPE which indicates the electron transfer kinetics become higher due to enhancement of conductivity and active surface.[31] The conductive polymer attached with g-C$_3$N$_4$ and decreased the value of ΔE_p (66 mV) by enhancing electron transfer efficiency.[24] The behavior of the proposed biosensor was also proved by EIS measurement in the supporting redox probe at a frequency ranging from 0.1 to 10^5 Hz with an amplitude of 10 mV. Fig. 2B shows the Nyquist plot of different modified electrodes which compare the semi-circles portion lying on the axis. A higher semi-circle exhibits higher electron transfer resistance (R_{ct}) due to the long charge transfer process.[3] The R_{ct} of g-C$_3$N$_4$/SPE is smaller than bare SPE that indicates g-C$_3$N$_4$ creates several active sites for electron transfer and enhances the conductivity of the modified electrode. Dramatically, the R_{ct} value of APTES/ g-C$_3$N$_4$/SPE was significantly decreased after attaching the conductive polymer to the surface of g-C$_3$N$_4$/SPE.

The effect of scan rate on the peak current of APTES/g-C$_3$N$_4$/SPE was confirmed by a series of CVs analyses of the supporting electrolyte at different scan rates of 10, 20, 30, 40, 50, 60, 70, 80, 90, 100 mV s^{-1} in the potential range of −0.2 V to 0.6 V which is shown in Fig. 2C and D. The results of the experiment show excellent linearity between the scan rate and oxidation (I_{pa}), and reduction (I_{pc}) peak current with satisfactory correlation coefficient (R^2) suggesting a mass transfer phenomena belonging to adsorption control process on the interface of APTES/g-C$_3$N$_4$/ SPE and solution.[32]

3.3 Optimization of experimental condition

To achieve the better performance of the proposed electrochemical biosensor, several parameters such as pH, amount of g-C$_3$N$_4$ used for drop-casting were optimized. To optimize the pH for detection of E2, a series of DPV of 1×10^{-7} mol L^{-1} E2 in supporting electrolyte at different pH ranging 5.5 to 8.5. Fig. 3A shows the pH-dependent peak current deviation behavior of E2
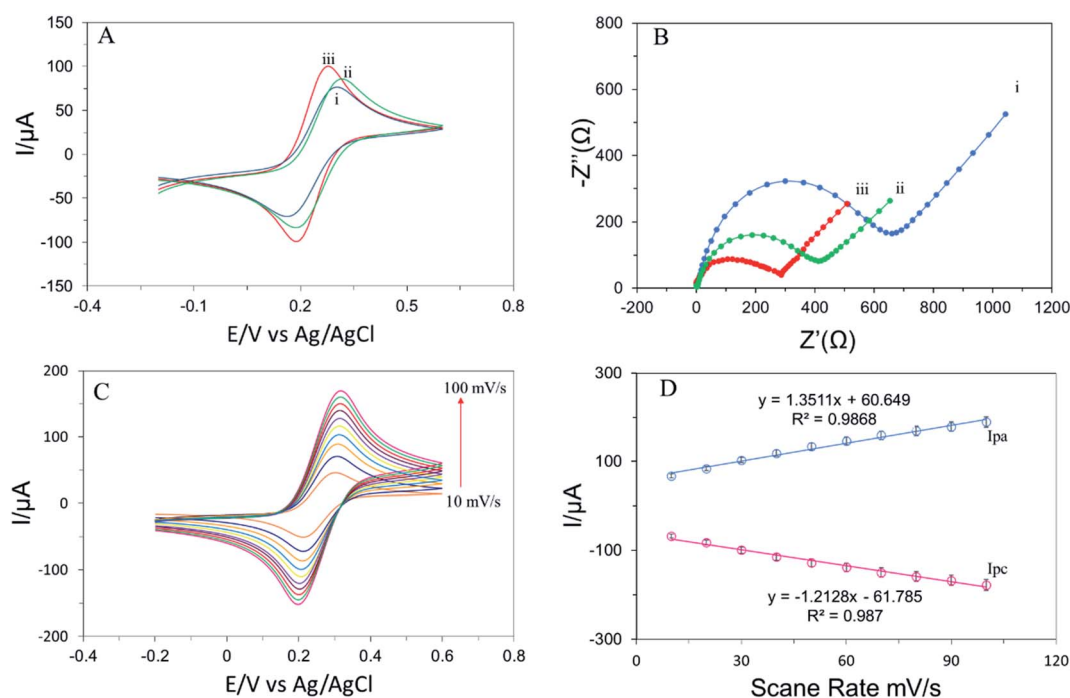

Fig. 2 (A) Cyclic voltammograms and (B) Nyquist plot of EIS of the different electrodes measured in 0.1 mol L^{-1} KCl including 5.0×10^{-3} mol L^{-1} [Fe(CN)$_6$]$^{3-/4-}$: (i) bare SPE, (ii) APTES/g-C$_3$N$_4$, (iii) APTES/g-C$_3$N$_4$/SPE. (C) CV response obtained for APTES/g-C$_3$N$_4$/SPE sensor at different scan rates (from inner to outer): 10, 20, 30, 40, 50, 60, 70, 80, 90 and 100 mV s^{-1} in 0.1 mol L^{-1} KCl including 5.0×10^{-3} mol L^{-1} [Fe(CN)$_6$]$^{3-/4-}$ and (D) the corresponding calibration plots between different scan rates *versus* anodic and cathodic peak current.
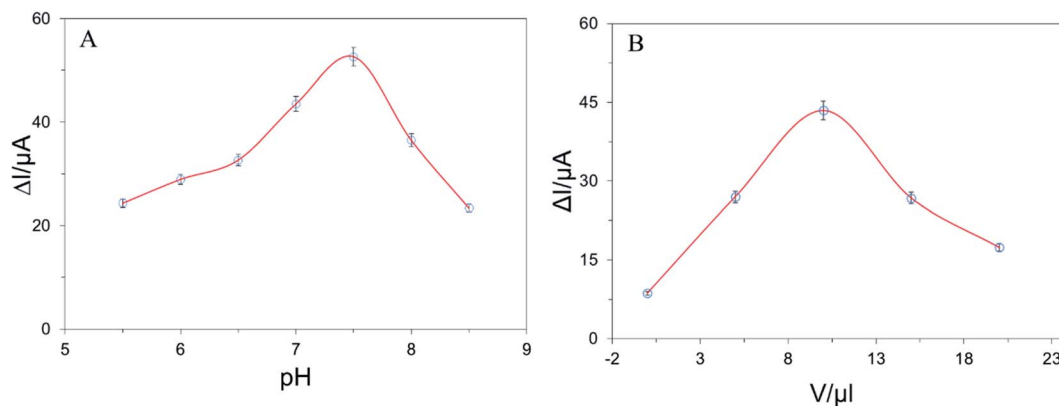
Fig. 3 (A) The effect of pH and (B) the volume of g-C_3N_4 used on current response performed with 1.0×10^{-9} mol L^{-1} E2.

(after and before adding E2). The highest peak current deviation was found at pH 7.0 indicating the highest amount of electron transfer occurred at neutral conditions. Fig. 3B represents the relationship between peak current deviation (after and before adding E2) and volume of g-C_3N_4 drop cast on the electrode surface. The current deviation value of E2 was rose consecutively by adding g-C_3N_4(0 to 10 μl) and become the highest for 10 μl drop-casting. Surprisingly, the peak deviation was fall for adding g-C_3N_4 furthermore due to the higher amount of g-C_3N_4 cover electrode surface and reduce electron transfer rate.

3.4   Analytical performance of the modified biosensor

The analytical performance of different modified electrodes was measured by recording the DPV of E2 in the supporting electrolyte. Fig. 4A depicts the current deviation (ΔI) of the different modified electrodes which was calculated from the oxidation peak current deviation of supporting electrolyte in the presence and absence of E2. APTES/g-C_3N_4/SPE shows a higher peak current deviation than g-C_3N_4/SPE and bare SPE. Fig. 4B represents the concentration-dependent DPV response of E2 which reveals the peak current decreased with increasing the

concentration of E2 suggesting the active sites of APTES/g-C_3N_4/SPE were almost occupied by E2.[15] The calibration curve in Fig. 4B expresses a linear relationship between ΔI and logarithm concentration of E2 in the range of 1×10^{-6} to 1×10^{-18} mol L^{-1} with an R^2 value of 0.9904. The limit of detection (LOD) was calculated as 9.9×10^{-19} mol L^{-1} from the signal–noise ratio (S/N = 3). Table 1 represents a comparison of LOD, wide range of linearity, and method adopted to detect E2 with some previously reported biosensors for detection of E2.[3,8,15,16,33–38]

3.5   Selectivity, reproducibility, and stability of electrochemical biosensor

The selectivity, reproducibility, and stability of a biosensor is the most important parameters to evaluate the practical application of the biosensor. The selectivity of the electrochemical biosensor was investigated by using the DPV current responses in the presence of similar structural compounds such as testosterone, progesterone, and naturally occurring substances such as some ions (Na$^+$, K$^+$, Ca^{2+}, Mg^{2+}, Fe^{2+}, Fe^{3+}, Al^{3+}, NO$_3^-$, SO$_4^{2-}$, Cl$^-$), glucose. Fig. 5A shows that the current responses ΔI
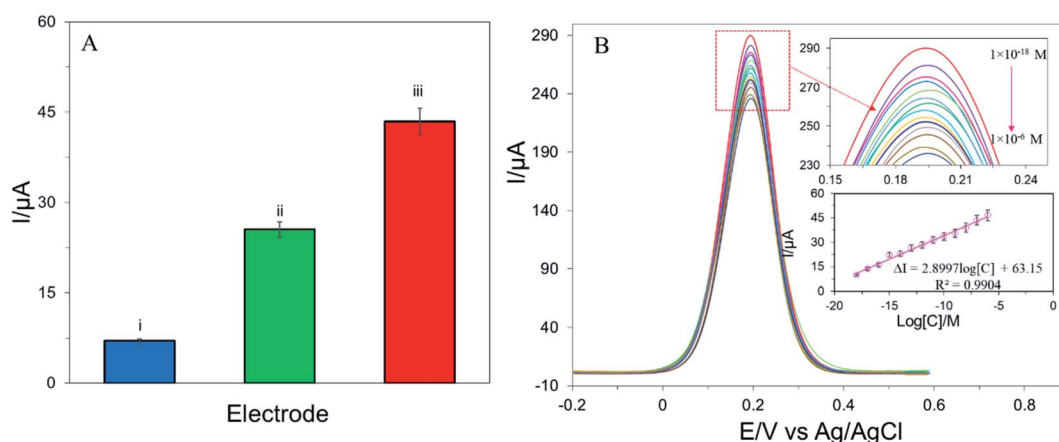
Fig. 4 DPV current response deviation (ΔI) of (i) bare SPE, (ii) g-C_3N_4/SPE and (iii) APTES/g-C_3N_4/SPE (A); DPV response curve of APTES/g-C_3N_4/SPE in 1×10^{-18} to 1×10^{-6} mol L^{-1} E2 in 5×10^{-3} mol L^{-1} [Fe(CN)$_6$]$^{3-/4-}$ containing 0.1 mol L^{-1} KCl and inserts shows the corresponding calibration curves of peak currents vs. logarithm of E2 concentrations (B).

Table 1 Comparison with previously reported sensor for detection of E2[a]

Electrode type	Electrochemical method	Dynamic range (mol L^{-1})	LOD (mol L^{-1})	Ref.
Pt/MWNTs/GCE	CV	1.8×10^{-12} to 5.5×10^{-11}	6.6×10^{-13}	33
MIS/PtNPs/GCE	DPV	3.0×10^{-8} to 5.0×10^{-5}	1.6×10^{-8}	34
MIPs/AuNPs/GCE	EIS	1.0×10^{-12} to 1.0×10^{-7}	1.8×10^{-12}	15
Aptamer/FNCP/GCE	EIS	1.0×10^{-15} to 1.0×10^{-6}	1.0×10^{-15}	35
GC/RGO/CuTthP	DPV	1.0×10^{-7} to 1.0×10^{-6}	5.3×10^{-9}	37
Fe$_3$O$_4$/MIP/SPCE	SWV	5.0×10^{-8} to 1.0×10^{-5}	2.0×10^{-8}	8
Poly(3,6-diamino-9-ethylcarbazole)/MIP/GCE	EIS	1.0×10^{-18} to 1.0×10^{-5}	3.6×10^{-18}	3
MIP/MIL-53/CNTs/GCE	DPV	1.0×10^{-14} to 1.0×10^{-9}	6.9×10^{-19}	36
Nanowell-based MIPs	EIS	1.0×10^{-12} to 1.0×10^{-5}	1.0×10^{-13}	1
g-C$_3$N$_4$/APTES/SPE	DPV	1.0×10^{-6} to 1.0×10^{-18}	9.9×10^{-19}	This work

[a] MWCNTs – multi wall carbon nanotubes, MIS – molecularly imprinted sensor, MIPs – molecularly imprinted polymers, FNCP – functionalised nanoporous conducting polymer, CuTthP: Cu(II)-*meso*-tetra(thien-2-yl)porphyrin, MIL-53 (AlO Hbdc, bdc = benzene-1,4-dicarboxylate).

of E2 was higher than others at same concentration (1×10^{-6} mol L^{-1}) by using the same electrode in the supporting electrolytic solution. This result evaluated that the electrochemical biosensor was good selectivity to recognize E2 molecules.

In practical application, reproducibility can play an important role for the APTES/g-C$_3$N$_4$/SPE based on the electrochemical biosensor. In this study, inter-assay and intra assay reproducibility was analysed according to standard methodology. To evaluate the intra-assay reproducibility and repeatability of electrochemical biosensor, the peak response of E2 in the supporting electrolyte was investigated by using $1 \times$

10^{-7} mol L^{-1}. After conducting five repetitive DPV response of same modified electrodes, the relative standard deviation was calculated as 1.18% which was shown in Fig. 5B. The inter-assay reproducibility was explored by conducting similar operation in E2 of different concentration. For a relative standard deviation (1.5%) was found which is reliable for biosensing application. The results of the experiment proved that the reproducibility of this sensor was satisfactory. Furthermore, the DPV response of E2 was obtained 97.6% and 95.24% after one- and two-weeks storage, respectively (Fig. 5C) while stored at 4 °C which indicates the biosensor is highly stable.
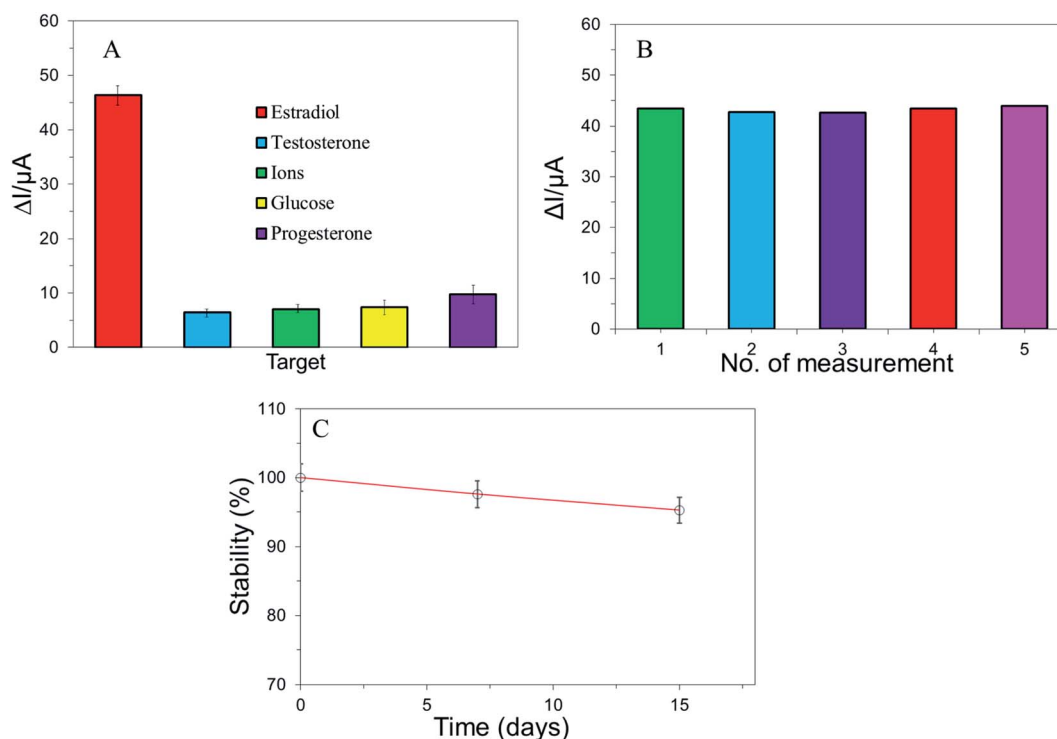

Fig. 5 Current response of deviation of E2, testosterone, progesterone, ions, glucose (A); reproducibility analysis through five repetitive measurements of E2 (B); stability profile of APTES/g-C$_3$N$_4$/SPE after storage periods (weeks) at 4 °C (C).

Table 2 Determination of E2 in real samples. ($n = 3$)

Sample type	Added (mol L^{-1})	Found (mol L^{-1}) (mean $\pm$ SD)	Recovery (%)
Milk	1.0×10^{-6}	$1.048 \pm 0.008 \times 10^{-6}$	104.8
	1.0×10^{-10}	$1.021 \pm 0.004 \times 10^{-10}$	102.1
	1.0×10^{-16}	$0.951 \pm 0.008 \times 10^{-16}$	95.1
Meat (poultry)	1.0×10^{-6}	$0.968 \pm 0.002 \times 10^{-6}$	99.8
	1.0×10^{-10}	$1.030 \pm 0.002 \times 10^{-10}$	103.0
	1.0×10^{-16}	$1.012 \pm 0.002 \times 10^{-6}$	101.2
Water	1.0×10^{-6}	$0.998 \pm 0.007 \times 10^{-6}$	96.8
	1.0×10^{-10}	$0.985 \pm 0.005 \times 10^{-10}$	98.5
	1.0×10^{-16}	$0.963 \pm 0.002 \times 10^{-16}$	96.3

3.6 Application of electrochemical biosensor in real food sample analysis

To access the practical application of the modified electrochemical biosensor, the biosensor was used to detect E2 in the spiked milk, meat and water sample *via* standard addition methods. DPV of 1×10^{-6} mol L^{-1}, 1×10^{-10} mol L^{-1} and 1×10^{-16} mol L^{-1} E2 was carried out in the presence of as prepared spiked real sample. The biosensor exhibits excellent recoveries ranging from 95.1% to 104.8% which is shown in Table 2. In addition, these results proved that the proposed biosensor shows high efficiency to detect E2 in food and environmental samples.

4 Conclusion

Conventional methods for screening E2 in food and environmental samples suffer from some drawbacks such as lack of selectivity, lack of sensitivity, time-consuming experimental procedure, expensive, and required trained operator. To overcome the arising problems, an advance electrochemical biosensor was developed to monitor E2 in environmental and food sample. The electrochemical biosensor is based on g-C$_3$N$_4$ and APTES modified SPE and used to identify E2 attomolar level with high selectivity and stability. The biosensor exhibits wide range of linearity from 1×10^{-6} to 1×10^{-18} mol L^{-1}. The biosensor was successfully applied to detect E2 in spiked milk, meat and water samples with excellent recoveries. So, the developed biosensor can detect E2 at the lowest limit with excellent selectivity, stability and sensitivity compare to the previously reported biosensor for detection E2. Thus, the design biosensor will be an effective tool for monitoring food quality and detecting of E2 in foodstuff and environmental contaminates.

Conflicts of interest

The authors declare that there is no conflict of interest in this work.

Acknowledgements

References

1 H. Pu, Z. Huang, D. W. Sun and H. Fu, *Crit. Rev. Food Sci. Nutr.*, 2019, **59**, 2144–2157.

2 B. Yilmaz and Y. Kadioglu, *Arabian J. Chem.*, 2017, **10**, S1422–S1428.

3 W. Liu, H. Li, S. Yu, J. Zhang, W. Zheng, L. Niu and G. Li, *Biosens. Bioelectron.*, 2018, **104**, 79–86.

4 W. Zhu, H. Peng, M. Luo, N. Yu, H. Xiong, R. Wang and Y. Li, *Food Chem.*, 2018, **261**, 87–95.

5 M. Pezzolato, C. Maurella, K. Varello, D. Meloni, C. Bellino, L. Borlatto, D. Di Corcia, P. Capra, M. Caramelli and E. Bozzetta, *Food Control*, 2011, **22**, 1668–1673.

6 X. Du, L. Dai, D. Jiang, H. Li, N. Hao, T. You, H. Mao and K. Wang, *Biosens. Bioelectron.*, 2017, **91**, 706–713.

7 X. Yao, Z. Wang, L. Dou, B. Zhao, Y. He, J. Wang, J. Sun, T. Li and D. Zhang, *Sens. Actuators, B*, 2019, **289**, 48–55.

8 A. A. Lahcen, A. A. Baleg, P. Baker, E. Iwuoha and A. Amine, *Sens. Actuators, B*, 2017, **241**, 698–705.

9 T. T. Schug, A. Janesick, B. Blumberg and J. J. Heindel, *J. Steroid Biochem. Mol. Biol.*, 2011, **127**, 204–215.

10 T. Tanaka, H. Takeda, F. Ueki, K. Obata, H. Tajima, H. Takeyama, Y. Goda, S. Fujimoto and T. Matsunaga, *J. Biotechnol.*, 2004, **108**, 153–159.

11 A. Peñalver, E. Pocurull, F. Borrull and R. M. Marcé, *J. Chromatogr. A*, 2002, **964**, 153–160.

12 A. Stafiej, K. Pyrzynska and F. Regan, *J. Sep. Sci.*, 2007, **30**, 985–991.

13 F. Regan, A. Moran, B. Fogarty and E. Dempsey, *J. Chromatogr. A*, 2003, **1014**, 141–152.

14 A. Azzouz and E. Ballesteros, *Food Chem.*, 2015, **178**, 63–69.

15 X. Zhang, Y. Peng, J. Bai, B. Ning, S. Sun, X. Hong, Y. Liu, Y. Liu and Z. Gao, *Sens. Actuators, B*, 2014, **200**, 69–75.

16 T. Wen, M. Wang, M. Luo, N. Yu, H. Xiong and H. Peng, *Food Chem.*, 2019, **297**, 124968.

17 Y. Li, X. Zhao, P. Li, Y. Huang, J. Wang and J. Zhang, *Anal. Chim. Acta*, 2015, **884**, 106–113.

18 T. B. Tran, S. J. Son and J. Min, *BioChip J.*, 2016, **10**, 318–330.

19 H. Medetalibeyoğlu, *Carbon Lett.*, 2021, **31**(6), 1237–1248.

20 G. Kesavan and S. M. Chen, *Microchem. J.*, 2020, **159**, 105587.

21 J. O. S. Silva, M. V. S. Sant'Anna, A. Gevaerd, J. B. S. Lima, M. D. S. Monteiro, S. W. M. M. Carvalho and E. Midori Sussuchi, *Electroanalysis*, 2021, 1–10.

22 M. L. Yola, T. Eren and N. Atar, *J. Electrochem. Soc.*, 2016, **163**, B588–B593.

23 M. Z. H. Khan, X. Liu, J. Zhu, F. Ma, W. Hu and X. Liu, *Biosens. Bioelectron.*, 2018, **108**, 76–81.

24 M. R. Ali, M. S. Bacchu, M. A. A. Setu, S. Akter, M. N. Hasan, F. T. Chowdhury, M. M. Rahman, M. S. Ahommed and M. Z. H. Khan, *Biosens. Bioelectron.*, 2021, **188**, 113338.

25 W. Zhang, Z. Zhao, F. Dong and Y. Zhang, *Chin. J. Catal.*, 2017, **38**, 372–378.

26 M. R. Ali, M. S. Bacchu, M. Daizy, C. Tarafder, M. S. Hossain, M. M. Rahman and M. Z. H. Khan, *Anal. Chim. Acta*, 2020, **1121**, 11–16.

27 M. Kim, S. Hwang and J. S. Yu, *J. Mater. Chem.*, 2007, **17**, 1656–1659.

28 S. Sunasee, K. H. Leong, K. T. Wong, G. Lee, S. Pichiah, I. W. Nah, B. H. Jeon, Y. Yoon and M. Jang, *Environ. Sci. Pollut. Res.*, 2019, **26**, 1082–1093.

29 A. R. Unnithan, A. R. K. Sasikala, P. Murugesan, M. Gurusamy, D. Wu, C. H. Park and C. S. Kim, *Int. J. Biol. Macromol.*, 2015, **77**, 1–8.

30 M. R. Ali, M. S. Bacchu, M. R. Al-Mamun, M. S. Ahommed, M. A. Saad Aly and M. Z. H. Khan, *RSC Adv.*, 2021, **11**, 15565–15572.

31 B. Sriram, J. N. Baby, Y.-F. Hsu, S.-F. Wang and M. George, *J. Electrochem. Soc.*, 2021, **168**, 087502.

32 M. Z. H. Khan, M. S. Ahommed and M. Daizy, *RSC Adv.*, 2020, **10**, 36147–36154.

33 X. Lin and Y. Li, *Biosens. Bioelectron.*, 2006, **22**, 253–259.

34 L. Yuan, J. Zhang, P. Zhou, J. Chen, R. Wang, T. Wen, Y. Li, X. Zhou and H. Jiang, *Biosens. Bioelectron.*, 2011, **29**, 29–33.

35 B. Zhu, O. A. Alsager, S. Kumar, J. M. Hodgkiss and J. Travas-Sejdic, *Biosens. Bioelectron.*, 2015, **70**, 398–403.

36 D. Duan, X. Si, Y. Ding, L. Li, G. Ma, L. Zhang and B. Jian, *Bioelectrochemistry*, 2019, **129**, 211–217.

37 F. C. Moraes, B. Rossi, M. C. Donatoni, K. T. de Oliveira and E. C. Pereira, *Anal. Chim. Acta*, 2015, **881**, 37–43.

38 K. Spychalska, D. Zając and J. Cabaj, *RSC Adv.*, 2020, **10**, 9079–9087.